



A01-34128

AIAA-2001-3353

**A Review of Spacecraft Material Sputtering
By Hall Thruster Plumes**

I. D. Boyd and M. L. Falk

University of Michigan

Ann Arbor, MI 48109.

AIAA Paper 2001-3353

AIAA 37th Joint Propulsion Conference, Salt Lake City, Utah, July 2001

A Review of Spacecraft Material Sputtering

By Hall Thruster Plumes

Iain D. Boyd* and Michael L. Falk†

University of Michigan

Ann Arbor, Michigan

Abstract

Sputtering of spacecraft surfaces by energetic xenon ions in the plumes of Hall thrusters is a primary integration concern. The available literature is surveyed to identify useful sources of information for estimating these effects. In particular, the search considers relevant experimental measurements, analytical theory, and computer modeling. Sputter yields have been measured at normal incidence caused by xenon ions incident on many single-element materials. However, for more complex materials used on spacecraft such as silicon dioxide and Kapton, no direct yield measurements with xenon have been made. There are many theoretical models available for the estimation of xenon sputter yields of single- and multi-element surfaces, but these are generally only reliable after direct calibration against experimental measurements. There are a number of well-established, public-domain computer codes for simulating ion sputtering processes that are based on a Binary Collision Approximation (BCA) or a Molecular Dynamics (MD) approach. The BCA codes are more numerically efficient but less physically accurate than the MD methods. These computational methods appear to offer the potential to generate data-bases of sputter yields for complex materials as a function of impact energy and angle.

1. Introduction

One of the main integration concerns in placing Hall thrusters on spacecraft is the possible sputtering of sensitive surfaces by the xenon ions. The sputtering can lead to unexpected changes in the thermal, optical, and electrical properties of the materials, and the sputtered material may become re-deposited on other spacecraft surfaces. There is therefore a strong requirement to understand in detail the physical mechanisms of xenon ions sputtering the materials used on spacecraft. The goal of this study is to perform literature surveys to identify information useful for estimating erosion effects on spacecraft materials due to sputtering by low energy (around 300 eV) xenon ions emitted by Hall thrusters. In this report we summarize our findings for:

- (a) Experimental studies and theoretical models;
- (b) Computer models and potential energy surfaces.

* Associate Professor. Department of Aerospace Engineering. iainboyd@umich.edu

† Assistant Professor. Department of Materials Science and Engineering

We focused our study on the following primary spacecraft materials:

- (i) elemental solids: carbon (graphite), aluminum, silver, and gold;
- (ii) multi-element solids: silicon dioxide, and Kapton.

We first review the literature on experimental measurements and theoretical models. This is followed by a review of computer simulations. The report is concluded with a summary and recommendations for future work.

2. Experimental Studies and Theoretical Models

There are many reports in the literature on measurements of sputtering phenomena. These have been conducted primarily in the physics and materials sciences communities. There are a number of very useful review articles on the subject.¹⁻³ The xenon ion energies produced by Hall thrusters being less than 1 keV fall into the category of low-energy, high-mass ion sputtering. We found only a very few studies that specifically considered xenon ion sputtering in the energy range of interest for Hall thrusters. Therefore, in the following sections, where appropriate, we also provide results for xenon sputtering from theoretical models that have been calibrated and assessed for other systems.

2.1 Yields at Normal Incidence

Yamamura and Tawara⁴ have gathered together a large volume of data for ion sputtering of monatomic solids at normal incidence. For xenon ions in the energy range of interest (300 eV), sputter yields are presented for C (graphite), Al, Ag, and Au from the original experiments of Rosenberg and Wehner.⁵ These data are listed in Table 1 and plotted in Fig. 1. Also included in Fig. 1 is a fit of the Ag data proposed by Pencil et al.⁶ using the following semi-empirical formula:

$$Y = s_0 E^{0.25} (1 - s_1/E)^{3.5} \quad (1)$$

where the fit coefficients for Ag have values of $s_0=0.792652$ and $s_1=42.5165$. This formula provides a reasonable description of the Ag data over the energy range of interest.

For reference, it should be noted that Ref. 4 provides xenon ion sputtering data in graphic form for the following elemental surfaces: Be, Si, Ti, V, Cr, Mn, Fe, Co, Ni, Cu, Ge, Zr, Nb, Mo, Ru, Rh, Pd, Sn, Hf, Ta, W, Re, Os, Ir, Pt, Th, and U. Reference 7 provides tabulated data for xenon ions sputtering Ag, Au, Cu, Fe, Ge, Mo, Ni, Pd, Si, Ti, and Zn. Yield data are plotted as a function of atomic number, Z , in Fig. 2 for xenon ion sputtering at 300 eV based on the data reported in Ref. 5. The main trend that can be discerned is the increase of yield with atomic number along each row of the periodic table. This is seen for Ti ($Z=22$) to Cu ($Z=29$), Zr ($Z=40$) to Ag ($Z=47$), and Hf ($Z=72$) to Au ($Z=79$).

Experimental measurements of the yield at normal incidence for sputtering of silicon dioxide by argon ions for energies between 3 and 40 keV are reported by Nenadovic et al..⁸ Bach⁹ provides a model for computing the yield of SiO_2 at normal incidence that over predicts the data of Ref. 8 by only 20% for argon.

In Bach's model, the overall yield is given by:

$$Y = \frac{K \sum_i c_i \alpha_i S_{ni}}{U_a/Z} \quad (2)$$

where $K=0.042 \text{ \AA}^{-2}$, U_a is the atomization energy per molecule (18.8 eV for SiO_2), and Z is the number of atoms in the molecule. The summation is performed over each of the elements i in the bulk material (Si and O in our case), where c_i is the atomic fraction, and

$$\alpha_i = 0.15 + 0.13 \frac{M_i}{M_p} \quad (3)$$

where M_i is the molecular weight of element i , and M_p is the molecular weight of the projectile ion (Xe in our case). The quantity S_{ni} is the cross section (eV \AA^2) for nuclear collisions given by:

$$S_{ni} = \frac{84.62 Z_p Z_i M_p s_n(\varepsilon)}{(M_p + M_i)(Z_p^{0.23} + Z_i^{0.23})} \quad (4)$$

where

$$s_n(\varepsilon) = \frac{\log(1 + 1.1383\varepsilon)}{2(\varepsilon + 0.01321\varepsilon^{0.21226} + 0.19593\sqrt{\varepsilon})} \quad (5)$$

and

$$\varepsilon = \frac{32.53 M_i E}{Z_p Z_i (M_p + M_i)(Z_p^{0.23} + Z_i^{0.23})} \quad (6)$$

In the above expressions, Z_i is the atomic number of element i , Z_p is the atomic number of the projectile ion (xenon in our case), and E is the ion energy in keV. Results obtained using the above model are shown in Fig. 3 for xenon ion energies of interest to Hall thruster sputtering. Based on the argon data, the model results are likely to be about 20% too high. Also shown in Fig. 3 are results obtained using Eq. (1) with the coefficients recommended for SiO_2 by Pencil et al.⁶: $s_0=0.18397$ and $s_1=92.125$. These coefficients were obtained by fitting the available data for sputtering of monatomic silicon. In comparing these two models, they provide reasonable agreement at high energy, particularly when the Bach model results are reduced by the 20% estimated over-prediction. However, the Bach model predicts essentially a zero threshold energy that is clearly incorrect. Further research is required to more accurately characterize the sputtering of SiO_2 at normal incidence.

Ferguson¹⁰ reports on sputtering of Kapton by oxygen ions at 5 eV and argon ions at 1,065 eV. The oxygen experiments are of interest for Space Shuttle flight conditions. For the argon experiments, it is stated that "no significant material loss or change of optical properties" was detected. Michael and Stulik¹¹ describe the sputtering of Kapton-H ($\text{C}_{22}\text{H}_{10}\text{N}_2\text{O}_5$) by 6,000 eV xenon atoms. The reported sputter yield is 0.08 Kapton units/atom which translates into 30 amu/atom. This can be compared to a yield of 75,000 amu/atom for Teflon sputtering at the same conditions. Hence, it is concluded that Kapton has a significantly smaller sputter yield than other polymers. Assuming a linear dependence of the sputter yield on impact energy (e.g. Eq. (14) of Ref. 3), the yield for Kapton at 300 eV impact energy of xenon ions is estimated to be 0.004 Kapton units/ion or 1.5 amu/ion. Fife et al.¹² report measurements of erosion of various materials

placed in the plume of the SPT-140 Hall thruster. Kapton erosion data are provided at angles of 35 and 60 deg. from the plume centerline at a distance of 1 m from the thruster. Using the measured erosion rates combined with ion current density data also reported in Ref. 12 at the same locations, the yields at these angles are estimated to be 0.0067 and 0.0049 Kapton units/ion, respectively. These values are quite close to the estimate obtained above from linear extrapolation.

Since the yield of a particular element in a multicomponent sample is inversely proportional to the mass of that element (Eq. (19) of Ref. 3), it is anticipated that hydrogen atoms are most likely to be sputtered first out of the Kapton, followed by carbon, nitrogen, and oxygen. With such preferential sputtering it is difficult to predict the effect of sputtering on the material properties of Kapton and the possible re-deposition of sputtered material on spacecraft surfaces.

2.2. Effects of Angle of Incidence

Angular distributions of sputter yield are reported in Ref. 1 for 1050 eV argon ions impacting on Al and Ag. No measured data were found relating directly to impingement of 300 eV xenon ions on the materials of interest. A useful analytical model for estimating the effects of angle of incidence on sputter yield was proposed by Yamamura¹³:

$$\frac{Y(\theta)}{Y(0)} = x^f \exp[-\Sigma(x - 1)] \quad (7)$$

where $Y(0)$ is the yield at normal incidence, $Y(\theta)$ is the yield at angle of incidence θ , $x=1/\cos(\theta)$, and f and Σ are parameters related by $\cos(\theta_{opt})=\Sigma/f$ where θ_{opt} is the angle of maximum sputter yield. In Ref. 13, Yamamura provides best fit values for f and θ_{opt} for a number of ion-material sputtering systems that include xenon ions and some of the metals we are interested in. The fitting is based on experimental measurements reported by Bay and Bohdansky¹⁴ and Takeuchi and Yamamura.¹⁵ Unfortunately, there are no data directly corresponding to xenon ions sputtering C, Al, Ag, or Au. However, the data fits of Ref. 13 illustrate some important points and we plot some of them here in Figs. 4–9. In Fig. 4, the model predictions for argon ions impacting on various metals at 1.05 keV are shown. The predictions for Al and Ag offer excellent agreement with the measured data shown in Ref. 1. Figures 5 and 6 show the values of f and θ_{opt} proposed by Yamamura¹³ for xenon ions at varying energy impacting on Cu. These data indicate that f increases significantly and θ_{opt} decreases as the ion energy is reduced. Figures 7 and 8 show the values of f and θ_{opt} proposed by Yamamura¹³ for noble gas ions at a fixed energy of 1.05 keV impacting on Cu. These data indicate that f increases and θ_{opt} decreases with molecular weight. By performing linear interpolations of the data provided by Yamamura, values of f and θ_{opt} are estimated for the sputtering of Al, Ag, and Au by xenon ions at 300 eV. The values obtained are listed in Table 2. The resulting yields for these metals are plotted in Fig. 9. These can only be considered gross estimates.

One of the main problems with the model of Yamamura is the significant variation in f at low energies. To account for this effect, Oechsner¹ proposed the following model:

$$\frac{Y(\theta)}{Y(0)} = \frac{A}{Y(0)} + 1 \quad (8)$$

where $Y(0)$ is the yield at normal incidence, and $Y(\theta)$ is the yield at angle of incidence θ . The property A is given by:

$$A = c \frac{\sigma}{d^2} \frac{\varepsilon E}{U_o} F(\theta') \quad (9)$$

where $c=0.0249$, σ is the hard sphere collision cross section between the incoming ion and a single element of the surface, d is the interatomic spacing in the surface material, E is the ion energy, U_o is the surface binding energy, $\varepsilon=4M_1M_2/(M_1+M_2)^2$, M_1 and M_2 are the masses of the ion and surface element, respectively. The function F is given as:

$$F(\theta') = 1.2 \left(\frac{\theta}{\theta_{opt}} \right)^2 \quad (10)$$

where θ_{opt} is the angle of maximum sputter yield. Table 3 lists the constants required to evaluate these equations for the elements of interest. Value of U_o were obtained from Ref. 16, values of θ_{opt} were obtained from plots shown in Ref. 1, and values of d were obtained from standard tables. For all systems, the value of σ was taken to be 2 \AA^2 as recommended in Ref. 1. Figure 10 plots the results where it can be seen that the increase in yield at angle of incidence is very high for graphite. Unfortunately, the model of Oechsner does not model the behavior just below and beyond the optimum sputtering angle therefore making it of limited use.

For completeness, comparison is made in Fig. 11 of the results for Au, Ag, and Al, between the models of Yamamura and Oechsner. There are significant differences between the predictions of these models clearly indicating this as an area where further work is required. Also shown in Fig. 11 are results due to Pencil et al.⁶ for silver where the following empirical formula is proposed:

$$\frac{Y(\theta)}{Y(0)} = 1 + c_o[1 - \cos(c_1\theta)]^{c_2} \quad (11)$$

and the coefficients for Ag are given as $c_0=0.42242$, $c_1=3.00$, and $c_2=0.78533$. Note that this expression has no dependence on the ion energy. This model offers reasonable agreement with the model of Yamamura at small angles, but behaves poorly at high angles.

Nenadovic et al.⁸ report data for the effect of incident angle on sputtering of silicon dioxide for argon ions in the energy range of 3 to 25 keV. The data for the lowest energy (3 keV) are plotted in Fig. 12 where we can see that $\theta_{opt}=50$ deg.. The data of Ref. 8 show a strong dependence on ion energy. Also shown in Fig. 12 are the data obtained using Eq. (11) above with the following coefficients proposed in Ref. 6: $c_0=1.153$, $c_1=2.852$, and $c_2=1.1131$. It is concluded that further research is required for xenon ions sputtering SiO_2 in the low energy range of interest here.

No literature were discovered describing experiments on the effects of angle of incidence on Kapton sputtering.

3. Computer Models

There has been extensive work on numerical simulation of sputtering that can provide estimates for yields as a function both of beam energy and angle of incidence. Since the field has been in development

for at least forty years we will not attempt an exhaustive review of the computational literature here, instead concentrating on recent publications and up to date software that may be useful in applying the understanding that has been developed in this subject area. For a detailed account of the earlier literature see the excellent and very readable review up to 1987 by Andersen.¹⁷

The simulation methods available differ from each other primarily with respect to the accuracy with which inter-atomic collisions are modeled. However, it is important to note that codes that more accurately model collisions are often time-intensive and can suffer from an inability to simulate sufficient numbers of collisions to produce reliable statistics. The accuracy of these simulations depends critically on the extent to which the many-body nature of the problem is modeled. Both the details of the inter-atomic interaction potential and the degree of realism used in modeling particle dynamics are crucial in this regard.

3.1 Binary Collision Approximation (Monte Carlo Methods)

There exist a number of codes which have been developed since the mid-1970's that rely on a binary collision approximation (BCA) to compute sputter yields in addition to implantation depths and other relevant quantities. These methods are sometimes also referred to as Monte Carlo methods and are implemented in codes such as TRIM/SRIM,¹⁸ MARLOWE,¹⁹ UT-MARLOWE,²⁰ TRIRS, DYTRIRS²¹ and others. Some of these codes are available in the public domain and they are widely utilized in the field. These BCA codes model projectile-target interactions and target-target interactions as a series of two-body interactions. Some of the codes assume essentially amorphous material (TRIM/SRIM) while others make an assumption that the target is a single crystal (MARLOWE). Polycrystalline samples can also be approximated using the crystal codes.²² Amorphous codes either consider a fixed mean free path between collisions or choose from an exponential distribution of distances. The average mean free path is determined from the number density of atoms in the target.

TRIM is one of the most widely used codes because it is fast compared to other codes and can treat a large number of projectile ions. TRIM, like all BCA codes, models the collision cascade as a series of binary collision events between a moving atom (1) and a stationary atom (2). In each event, the impact parameter is chosen in a stochastic manner. Then the energy transfer in the collision is computed. Once the energies of the two atoms are known, these energies are compared to some simulation parameters: the displacement energy, E_d , the binding energy of an atom to its site, E_b , the surface binding energy, E_s , and the final energy after which the atom is no longer traced, E_f . If the energy after the collision of the originally stationary atom, E_2 , is greater than the displacement energy, E_d , then the atom is dislodged from its site and continues to travel with energy $E_2 - E_b$. Otherwise, the stationary atom will dissipate its energy as phonons. If the energy of the originally moving atom after the collision, E_1 , is also greater than E_d , then the moving atom also continues to collide and a vacancy is created. If, however, E_1 is less than E_d , then atom 1 takes the place of atom 2 causing either a replacement collision (if atoms 1 and 2 are of the same type) or an interstitial defect. The excess energy in either case is assumed to dissipate via phonons. If, however, both E_1 and E_2 are less than E_d , then atom 1 becomes an interstitial defect and all the energy is released as phonons. If an

atom is given sufficient energy to cross the surface it may sputter, but only if its kinetic energy normal to the surface exceeds the surface binding energy, E_s , of the target material.

As would be expected the results of a TRIM simulation depend quite sensitively the potential used to calculate the collision events *and* the various energetic parameters used. Many of these parameters are known only for a very small number of possible targets. The sputtering yield in particular is very sensitive to the surface binding energy, usually taken to be approximately the heat of sublimation, and is also sensitive to the lattice binding energy, E_b , that is not explicitly known for most compounds. The TRIM program contains a table of suggested values for the surface binding energies. In addition, the TRIM program has no way of including effects of surface roughness and changes in surface stoichiometry that may occur during sputtering.

TRIM has been used in the space propulsion field to model xenon ions from 100-1000 eV interacting with aluminum, stainless steel and graphite.²³ It is not clear from the literature, however, that the predictions of this code have been rigorously tested against relevant experimental data for Xe sputtering of spacecraft materials.

TRYRIS, another BCA code, allows multiple-atom interaction in an attempt to improve results at low energy.²¹ Using this technique, good agreement was obtained between experiment and simulation for Al and Si sputtering from doped GaAs structures and for yield during Ar sputtering of Cu, Ni and Ge targets. Closer agreement to experiment was reported by the authors of this code than was obtained using TRIM-95.

3.2 Molecular Dynamics Simulations

Molecular dynamics (MD) simulations do not make a binary collision assumption, but instead consider the motion and interactions of all the particles in the system including simultaneous interactions amongst many particles. As such, MD simulations, like the BCA simulations, make approximations via their choice of inter-atomic potentials, but realistically treat particle dynamics using a numerical scheme to integrate Newton's equations of motion. For this reason, MD simulations do not depend on a large number of arbitrary energetic cutoffs as in the BCA simulations. This technique, however, requires the existence of reliable potentials for the atomic interactions in question, an issue that will be discussed in more depth below. MD simulations automatically include interactions of an incident ion with multiple particles that may be particularly important for accurately simulating low-energy events. In addition, MD simulations explicitly model temperature effects because molecular vibrations (phonons) are simulated directly.

The most significant drawback of MD techniques is that they are very time intensive, and when more accurate potentials are used the time for the computation of a single collision cascade simulation can be significant. It is only recently with state-of-the-art computing facilities that MD simulations using fairly accurate potentials have been able to produce statistics that can be compared to experimental data directly. This is particularly a problem if the surface involved is not a predetermined single crystal facet, i.e. if averaging over different crystal orientations is necessary as in a polycrystal. Some of these cases will be discussed further below. However, it is important to note that MD simulations have been quite effective in

elucidating particular physical processes that occur during sputtering. Recent work has suggested that the binary collision paradigm may be inappropriate for modeling some of the processes that go on during ion irradiation.²⁴ In particular, the predicted damage in Si due to high mass ions has been reported to be higher in MD simulations than would be predicted using the BCA approximation.²⁵

3.3 Hybrid methods

Recently, Beardmore and Gronbeck-Jensen have pioneered an intermediate path between BCA and MD by developing reduced molecular dynamics schemes that consider interactions using molecular dynamics techniques but with reduced simulation cells that track each energetically excited atom, explicitly simulating a small number of the surrounding atoms.²⁶ As such, the computational time needed to track collision cascades is greatly reduced relative to a full MD simulation. As with MD simulations in general, the number of parameters needed to define the materials are greatly reduced relative to BCA if inter-atomic potentials are well developed.

3.4 Interaction Potentials

Choosing inter-atomic interaction potentials for sputtering simulations is crucial for accurate prediction of energy transfer during collisions. Because the reliable modeling of high-energy collision processes is critical to sputtering calculations, potential development in this field has focused on accurate response at small inter-nuclear separations. This is a different focus from studies of defects in solids where the behavior near the potential minima in the bulk and near surfaces is the most important aspect of the interaction. Thus, many of the potentials designed to model collisions in BCA type simulations are unsuited for use in MD calculations without modification, and typical MD potentials that are used to model low-energy processes inaccurately model collisions and other high-energy events. A typical fix is to create a hybrid potential that fits a standard low-energy potential near the energetic minimum and fits a high-energy potential at short inter-nuclear separation. However, for accurate MD calculations these potentials must also produce accurate estimates of dimer energies in addition to binding energies in bulk environments. This is often not the case for potentials designed solely for use in bulk and surface simulations. This issue has been recently addressed in some of the work that will be discussed below.

BCA simulations typically use screened Coulomb interactions of the Bohr type, such as the Moliere approximation to the Thomas-Fermi screened potential²⁷ (standard in MARLOWE¹⁹). These potentials are of a general electrostatic repulsive form with an additional term added to model the electronic screening over a *screening radius*, a :

$$V(r) = \frac{Z_1 Z_2 e^2}{r^2} \chi(r/a)$$

The various high-energy potentials differ only in the form of the screening function, χ and the value of a . The Moliere potential is a universal form for this screening function, χ , independent of the atomic species involved combined with a screening length, a , determined knowing the atomic numbers of the species involved in the collision. This potential does a reasonably good job of capturing interactions at small inter-nuclear distances

but has been shown to underestimate the screening effect. Therefore, most applications of this potential actually use a modified form that corrects for this underestimation.²⁸ The TRIM/SRIM computer code and other computational investigations make use of the ZBL potential²⁹ that is a parameterization of the same form as the Moliere potential but which takes into account a more accurate estimate of the screening length. However, the ZBL potential, like the Moliere potential, is an attempt to parameterize one potential to fit all possible atomic species with a universal form. As such, these universal potentials are not as accurate as potentials that are fit to data specific to the particular species being modeled.

Recent calculations comparing these empirical potential forms to *ab initio* quantum mechanical calculations show that the ZBL potential can be off by factors of 5-10% in the region of interest for accurate scattering calculations.³⁰ This is not surprising given the general nature of the potential and the fact that the ZBL potential is an attempt to fit a wide range of interactions with a single curve. However, in the context of any particular system, more accurate approximations to the potential can be obtained using density functional theory or other quantum mechanical methods. More recent versions of UT-MARLOW and SRIM utilize pair-specific interaction potentials where they are known either experimentally or theoretically.^{31,32}

Early work in the field all suffers from a reliance on central pair-potentials to model interactions. The most basic consequence of pair-potential formulations includes an inability to describe the binding energies of ejected clusters accurately. For MD calculations, central pair potentials have an additional drawback that they cannot model monatomic solids that have equilibrium crystal structures other than fcc. In addition to these shortcomings, pair-potentials do not take into account electron gas screening effects in metals and other surface phenomena that may strongly affect sputter yield. BCA calculations often get around the latter by including a potential barrier that must be overcome for an ion to separate from the surface as in the TRIM algorithm described above. In this sense, BCA calculations using pair-potentials may be better models of sputtering than pair-wise interacting MD models, but models based on these potentials cannot be relied on to provide yields to better than 20-30% accuracy, particularly at low energies.

A good deal of effort has gone into designing empirical potentials that are suitable for non-fcc crystal structures and for modeling materials surfaces and defects. Among these, the EAM potentials are the most often used potentials for modeling metals. EAM potentials depend not only on pair-wise interactions, but also on a local density parameter that characterizes the local environment, i.e. the local electronic density. These potentials have also been used in modeling sputtering with results better than those obtained in pair-wise interacting systems.^{33,34,35} However, EAM potentials are primarily fitted to low energy data (e.g. binding energies, elastic constants, thermal expansion coefficients) and do not properly model interactions at short inter-nuclear separations. For this reason, the EAM potentials are sometimes hybridized with ZBL potentials at short-range.³⁶ In addition, EAM potentials can overestimate the energies of dimers and other ejected clusters by a factor of 2.

Corrected effective medium (CEM) potentials have been used recently to model low energy (3 keV) Ar sputtering in metallic systems (Cu, Rh and Ni).^{37,38} These potentials consider both a pair-wise sum

of Coulombic interactions calculated from electron densities determined via Hartree-Fock calculations, and an interaction with a “jellium density” that enters into an empirical embedding function which allows the model to consider local environments ranging from the bulk to diatomic clusters.³⁹ This embedding function is adjusted to model the appropriate interaction energies and is not obtained from first principles. The main advantage of the CEM potentials is that they are reasonably accurate at small inter-nuclear separations. This is an advantage over EAM potentials and reasonable agreements with experimental data were observed using sets of 150 collisions to provide statistical information on the 450-500 ejected atoms. These simulations have proved useful in identifying mechanisms responsible for particular features in the angular distributions of sputtered particles from single crystal surfaces. However, they have been less accurate in predicting yield from polycrystalline samples, e.g. from Cu.⁴⁰

3.5 Inelastic Effects (Electronic Stopping)

One of the most difficult physical processes to include in sputtering simulations is inelasticity due to ion/electron interactions. This is sometimes referred to as “electronic stopping.” This effect becomes less important at low energy but can be important even as low as 10 eV particularly for light ions and in crystalline targets. However, even for heavy ions this effect is difficult to estimate and may decrease sputtering predictions by as much as 20%.¹⁶ These effects are generally not included in the potential and must be included in an effective way if they are included at all. Recent versions of UT-MARLOWE include an effective inelastic loss term.³¹

3.6 Angular Distributions

Both BCA and MD models can be used to obtain angular distribution data for sputtering yields, however the reliability of either method is subject to question. For BCA, as mentioned previously, the sputter yields predicted are quite sensitive to several of the input parameters that are not generally known *a priori*. In addition, the particular shape of the binding surface can significantly affect the predicted sputtering yields. Not surprisingly, BCA models with non-planar binding surfaces generally produce anisotropies, while planar surface barriers produce cosine-like flux.¹⁷ In the end, this discrepancy arises because BCA models do not handle surface molecules realistically. While both MD and BCA models can produce anisotropic yields, MD tends to predict more anisotropic yields than BCA. However, MD models suffer from the limited amount of data generated due to their computational intensity. Often these simulations focus on perfectly flat and well-defined crystal surfaces, while the surface of interest technologically may be polycrystalline and significantly roughened due to surface treatments and the sputtering process itself. However, as previously noted, recent state-of-the-art treatments of single crystal surfaces have produced reasonable comparisons to experimental data in certain metal systems.^{37,38}

4. Summary and Conclusions

4.1 Experimental Studies and Theoretical Models

Experimental measurements are available in the literature for xenon sputtering of the following elemental solids at normal incidence in the energy range of interest: Be, Si, Ti, V, Cr, Mn, Fe, Co, Ni, Cu, Ge, Zr, Nb, Mo, Ru, Rh, Pd, Sn, Hf, Ta, W, Re, Os, Ir, Pt, Th, U, and Zn.^{4,7} No measured data were found in the literature for sputtering of SiO₂ at normal incidence. However, the theoretical model of Bach⁸ and the empirical formula of Pencil et al.⁶ (based on sputtering of Si) for SiO₂ were found to be in reasonable agreement (see Fig. 3). Estimates obtained for Kapton indicated values of about 0.004 for the sputter yield for xenon at 300 eV.

The effect of angle of incidence on sputter yield for xenon ions could only be found for Cu.¹⁴ Using these data, combined with measured values for argon ions sputtering on various metals,^{14,15} the model of Yamamura¹³ (see Eq. 7), was employed to provide estimates of the effects of angle of incidence for sputtering of Ag, Au, and Ag (see Fig. 9) at 300 eV. The effect of angle of incidence on sputtering of SiO₂ has only been investigated experimentally for argon ions at 3,000 eV and the trend is in reasonable agreement with an empirical formula of Pencil et al.⁶ except at large angles (see Fig. 12).

4.2 Computer Models

It is the opinion of the authors that progress in modeling sputtering will require the development of a better connection between the various models currently employed. While MD simulation is unlikely to replace BCA models because of the time-intensive nature of the MD simulation, MD simulation may be useful in determining the meaning and quantitative value of some of the ill-defined but very important parameters upon which BCA models rely, in particular the various energetic parameters. In addition, use of density functional methods and other quantum mechanical techniques may be useful for determining interaction potentials accurately without having to extract them from experimental data. To accomplish this, it will be necessary to reconsider BCA models in order to devise a more rigorously well-determined coarse-grained physical picture, so that firm connections between simulation methodologies can be established. Currently, BCA models have become rather generous in the number of ill-determined parameters they employ leading to the situation where very impressive fits to the observed data can be obtained once the parameters are determined from the aforementioned data. Unfortunately, this is necessarily accompanied by a corresponding lack of predictive ability.

The authors, while recognizing that newer MD methods hold out the promise of a more complete understanding of sputtering, realize that these methods are unlikely to provide short-term answers to many of the questions relevant to current spacecraft engineering needs. For this reason, it is recommended that BCA codes (most likely SRIM2000) be used in order to extend the range and applicability of experimental sputtering data obtained directly from relevant materials systems. This will require that experiments be designed to extract the relevant energetic parameters for each material system of interest. Inter-particle potentials can be obtained either from the literature or from quantum mechanical calculations using density

functional theory or other similar methods. In this way, a few experimental investigations can be used to predict sputter yields in a variety of geometries and operational conditions without an extensive and time-consuming research effort. It is important to realize the limitations of this approach and to understand that such codes may be subject to reliabilities only within 10-30% or so. While such an approach will provide immediate benefit as input to an engineering effort, long term improvements in computational predictions will require investing research effort into the development of more physics-based continuum models that can be linked directly to MD and quantum mechanical simulation techniques.

4.3 Recommendations for Further Work

In terms of elemental solids, the main omission from the available literature is the study of the effects of angle of incidence on sputtering by xenon ions at 300 eV. In this study, a combination of data for xenon ion sputtering of copper and argon ion sputtering of Ag, Al, and Au, was used to develop a model of xenon sputtering of these elements (Fig. 9). However, it is not even possible at this stage to estimate the uncertainty in the model. It is therefore recommended that a computer simulation investigation be conducted (using a BCA code such as SRIM2000) to study angle of incidence effects on sputter yield for the elemental solids of interest (graphite, silver, aluminum, and gold). The physical parameters required for the computer simulations can be established using the measured data for sputtering of these materials at normal incidence.

There is no data for xenon sputtering of SiO₂ in the literature. However, the data measured for argon ion sputtering at 3 keV could again be used as the foundation of a computer simulation investigation to study the sputtering of SiO₂ by xenon ions at 300 eV. These simulations would most likely employ a BCA code such as SRIM2000.

For other materials of interest, if there is no data available in the literature, the overall procedure that we recommend is to perform (or have performed) a small number of experimental studies. These data can be used to establish the physical parameters required by the computer models that can subsequently be used to extend the data base for each system as needed.

This investigation has focused on the probability of erosion of spacecraft materials due to xenon ion impact. A related issue of significance in spacecraft integration is the directional scattering of the sputtered material that may become re-deposited on other spacecraft surfaces causing further degradation of performance. Once again, computer simulations offer a reasonable balance between accuracy and cost in addressing this issue. Either BCA or MD can be used and the question of accuracy is similar to that for predicting sputter yield. Namely, that BCA is more computationally efficient but not so well founded physically, while MD is more physically accurate if a suitable potential is available, but then is numerically expensive. It is therefore further recommended that a BCA computer investigation be conducted to generate data-bases of angular distributions for materials of interest as they are sputtered by xenon ions. This information could then be used in contamination studies of spacecraft configurations. The computer study must be performed in conjunction with an additional literature search to identify measured data sets that can be used to validate the computational models.

Acknowledgments

This work was funded by the Air Force Research Laboratory, Edwards Air Force Base, with Dr. Michael Fife as the monitor.

References

- ¹ Oechsner, H., "Sputtering - a Review of Some Recent Experimental and Theoretical Aspects," *Applied Physics*, Vol. 8, 1973, pp. 185-198.
- ² *Sputtering by Particle Bombardment 1. Physical Sputtering of Single Element Solids*, Edited by R. Behrisch, Springer-Verlag, New York, 1981.
- ³ Smentkowski, V.S., "Trends in Sputtering," *Progress in Surface Science*, Vol. 64, 2000, pp. 1-58.
- ⁴ Yamamura, Y. and Tawara, H., "Energy Dependence of Ion-Induced Sputtering Yields From Monatomic Solids at Normal Incidence," *Atomic Data and Nuclear Data Tables*, Vol. 62, 1996, pp. 149-253.
- ⁵ Rosenberg, D. and Wehner, G.K., "Sputtering Yields for Low Energy He⁺, Kr⁺, and Xe⁺ Ion Bombardment," *Journal of Applied Physics*, Vol. 33, 1962, pp. 1842-1845.
- ⁶ Pencil, E.J., Randolph, T., and Manzella, D.H., "End-of-Life Stationary Plasma Thruster Far-Field Plume Characterization," AIAA Paper 96-2709, July 1996.
- ⁷ Chambers, G.P. and Fine, J., "Pure Element Sputtering Yield Data," in *Practical Surface Analysis: Ion and Neutral Spectroscopy*, edited by D. Briggs and M.P. Seah, Wiley, New York, 1992, p. 705.
- ⁸ Nenadovic, T., Peraillon, B., Bogdanov, Z., Djordjevic, Z., and Milic, M., "Sputtering and Surface Topography of Oxides," *Nuclear Instruments and Methods in Physics Research*, Vol. B48, 1990, pp. 538-543.
- ⁹ Bach, H., "Ion Beam Sputtering of Silicate Glasses and Oxides," *Journal of Non-Crystalline Solids*, Vol. 102, 1988, pp. 36-42.
- ¹⁰ Ferguson, D.C., "Laboratory Studies of Kapton Degradation in an Oxygen Ion Beam," NASA Conference Publication, No. 2359, 1985, pp. 81-90.
- ¹¹ Michael, R. and Stulik, D., "A Semidynamic Study of Polymer Surface Morphology Development in Kapton-H Sputter Etched by 6 keV Xenon Atoms," *Nuclear Instruments and Methods in Physics Research*, Vol. B28, 1987, pp. 259-263.
- ¹² Fife, J.M., Hargus, W.A., Jaworske, D.A., Jankovsky, R., Mason, L., Sarmiento, C., Snyder, J.S., Malone, S. Haas, J., and Gallimore, A.D., "Spacecraft Interaction Test Results of the High Performance Hall System SPT-140," AIAA Paper 2000-3521, July 2000.
- ¹³ Yamamura, Y., "An Empirical Formula for Angular Dependence of Sputtering Yields," *Radiation Effects*, Vol. 80, 1984, pp. 57-72.
- ¹⁴ Bay, H.L. and Bohdansky, "Sputtering Yields for Light Ions as a Function of Angle of Incidence," *Journal of Applied Physics*, Vol. 19, 1979, pp. 421-426.
- ¹⁵ Takeuchi, W. and Yamamura, Y., "Computer Studies of the Energy Spectra and Reflection Coefficients of Light Ions," *Radiation Effects*, Vol. 71, 1983, pp. 53-64.

- ¹⁶ Gschneidner, K.A., "Physical Properties and Interrelationships of Metallic and Semimetallic Elements," in *Solid State Physics: Advances in Research and Applications*, edited by F. Seitz and D. Turnbull, Academic Press, New York, 1964, p. 276.
- ¹⁷ Andersen, H.H., "Computer Simulations of Atomic Collisions in Solids with Special Emphasis on Sputtering," *Nuclear Instruments and Methods in Physics Research*, Vol. B18, 1987, pp. 321–343.
- ¹⁸ Biersack, J.P. and Haggmark, L.G., "A Monte-Carlo Computer-Program for the Transport of Energetic Ions in Amorphous Targets," *Nuclear Instruments and Methods in Physics Research*, Vol. 174, 1980, pp. 257–269; Biersack, J.P. and Eckstein, W., "Sputtering Studies With the Monte Carlo Program TRIM," *Applied Physics A*, Vol. 34, 1984, pp. 73–94.
- ¹⁹ Robinson, M.T., Torrens, I.M., "Computer Simulation of Atomic-Displacement Cascades in Solids in the Binary-Collision Approximation," *Phys. Rev. B*, Vol. 9, 1974, pp. 5008–5024.
- ²⁰ Tian, S.Y., Morris, M.F., Morris, S.J., Obradovic, B., Wang, G., Tasch, A.F. and C.M., "A Detailed Physical Model for Ion Implant Induced Damage in Silicon," *IEEE Transactions on Electronic Devices*, Vol. 45, 1998, pp. 1226–1238.
- ²¹ Ber, B.J., Kharlamov, V.S., Kudrjavitsev, Yu.A., Merkulov, A.V., Trushin, Yu.V. and Zhurkin, E.E., "Computer Simulation of Ion Sputtering of Polyatomic Multilayered Targets," *Nuclear Instruments and Methods in Physics Research B*, Vol. 127/128, 1997, pp. 286–290.
- ²² For example Hou, M., and Robinson, M.T., "Computer Studies of Low Energy Scattering in Crystalline and Amorphous Targets," *Nuclear Instruments and Methods in Physics Research*, Vol. 132, 1976, pp. 641–645.
- ²³ Lutfy, F.M., Vargo, S.E., Muntz, E.P., Ketsdever, A.D., "A Cryogenically Pumped Space Simulation Facility for Plume and Contamination Studies," *Proceedings of the 18th Aerospace Testing Seminar*, Manhattan Beach, CA, March 16–18, 1999.
- ²⁴ Nordlund, K., Keinonen, J., Ghaly, M., Averback, R.S., "Coherent Displacement of Atoms During Ion Irradiation," *Nature*, Vol. 398, 1999, pp. 49–51.
- ²⁵ Caturla, M.J., delaRubia, T.D., Marques, L.A., Gilmer, G.H., "Ion-beam Processing of Silicon at keV Energies: A Molecular-Dynamics Study," *Physical Review B*, Vol. 54, 1996, pp. 16683–16695.
- ²⁶ Beardmore, K.M. and Gronbech-Jensen, N., "Efficient Molecular Dynamics Scheme for the Calculation of Dopant Profiles Due to Ion Implantation," *Physical Review E*, Vol. 57, 1998, pp. 7278–7287; "An Efficient Molecular Dynamics Scheme for Predicting Dopant Implant Profiles in Semiconductors," *Nuclear Instruments and Methods in Physics Research B*, Vol. 153, 1999, pp. 391–397.
- ²⁷ Moliere, G. Z., *Naturforsch*, Vol. 2a, 1947, pp. 133.
- ²⁸ O'Connor, D.J. and MacDonald, R.J., "A Correction Factor to the Interatomic Potential Screening Function for Use in Computer Simulations," *Radiation Effects*, Vol. 34, 1977, pp. 247–250.
- ²⁹ Ziegler, J. F., Biersack, J. P. and Littmark, U., *The Stopping and Range of Ions in Solids*, (Pergamon Press), New York, 1985; Williams, R.S., "Quantitative Intensity Analysis of Low-energy Scattering and

Recoiling from Crystal Surfaces,” in *Low Energy Ion-Surface Interactions*, ed. J.W. Rabalais, (Wiley), Chichester, 1994.

³⁰ Norlund, K., Runeberg, N., Sundholm, D., “Repulsive Interatomic Potentials Calculated Using Hartree-Fock and Density-Functional Theory Methods,” *Nuclear Instruments and Methods in Physics Research B*, Vol. 132, 1997, pp. 45-54.

³¹ Klein, K.M., Park, C. and Tasch, A.F., “Monte Carlo Simulation of Boron Implantation into Single-Crystal Silicon,” *IEEE Transactions on Electronic Devices*, Vol. 39, 1992, pp. 1614-1621.

³² SRIM webpage <http://www.research.ibm.com/ionbeams/SRIM/SRIMNOTE.HTM>.

³³ Bernardo, D. N. , Bhatia, R. and Garrison, B. J., “keV Particle Bombardment of Solids: Molecular Dynamics Simulations and Beyond,” *Computers in Physics Communications*, Vol. 80, 1994, pp. 259-273.

³⁴ Wucher, A., Watgen, M., Moessner, C., Oechsner, H. and Garrison, B. J., “Energy Dependent Studies of Anisotropic Atomic Sputtering of Nickel {111 },” *Nuclear Instruments and Methods in Physics Research B*, Vol. 67, 1992, pp. 531-535.

³⁵ Wucher, A., Garrison, B.J., “Internal and Translational Energy of Sputtered Silver Dimers: A Molecular Dynamics Study,” *Nuclear Instruments and Methods in Physics Research B*, Vol. 67, 1992, pp. 518-522.

³⁶ Wucher, A., Garrison, B.J., “Sputtering of Silver Dimers: A Molecular Dynamics Calculation Using a Many-Body Embedded-Atom Potential,” *Surface Science*, Vol. 260, 1992, pp. 257-266.

³⁷ Wucher, A., Garrison, B.J., “Cluster Formation in Sputtering: A Molecular Dynamics Study Using the MD/MC-Corrected Effective Medium Potential,” *Journal of Chemical Physics*, Vol. 105, 1996, pp. 5999-6007.

³⁸ Rosencrance, S.W., Burnham, J.S., Sanders, D.E., He, C., Garrison, B.J., Winograd, N., Postawa, Z., DePristo, A.E., “Mechanistic Study of Atomic Desorption Resulting From keV-Ion Bombardment of fcc {001} Single-Crystal Metals,” *Physical Review B*, Vol. 52, 1995, pp. 6006-6014.

³⁹ Stave, M.S., Sanders, D.E., Raeker, T.J. and DePristo, A.E., “Corrected Effective Medium Method. V. Simplifications for Molecular Dynamics and Monte Carlo Simulations,” *Journal of Chemical Physics*, Vol. 93, 1990, pp. 4413-4426.

⁴⁰ Colla, Th.J., Urbassek, H.M., Wucher, A., Staudt, C., Heinrich, R., Garrison, B.J., Dandachi, C., Betz, G., “Experiment and Simulation of Cluster Emission From 5keV Ar->Cu,” *Nuclear Instruments and Methods in Physics Research B*, Vol 143, 1998, pp. 284-297.

Table 1. Elemental yields for xenon ions impacting at normal incidence.

Energy (eV)	Al	Ag	Au	Graphite
100	0.06	0.40	0.16	0.00
200	0.24	1.05	1.00	0.04
300	0.45	1.80	1.83	0.08
600	1.02	4.20	3.10	0.21

Table 2. Parameters for xenon ion sputtering using the model of Yamamura.¹³

Element	f	θ_{opt} (deg)
Al	9.5	57.5
Ag	6.8	52.2
Au	6.8	49.0

Table 3. Parameters for xenon ion sputtering using the model of Oechsner.¹

Element	U_o (eV)	θ_{opt} (deg)	ϵ	d (Å)
Al	3.36	57.5	0.5656	2.82
Ag	2.97	52.2	0.9904	2.88
Au	3.80	49.0	0.9600	2.88
C (graphite)	7.42	60	0.3069	1.42

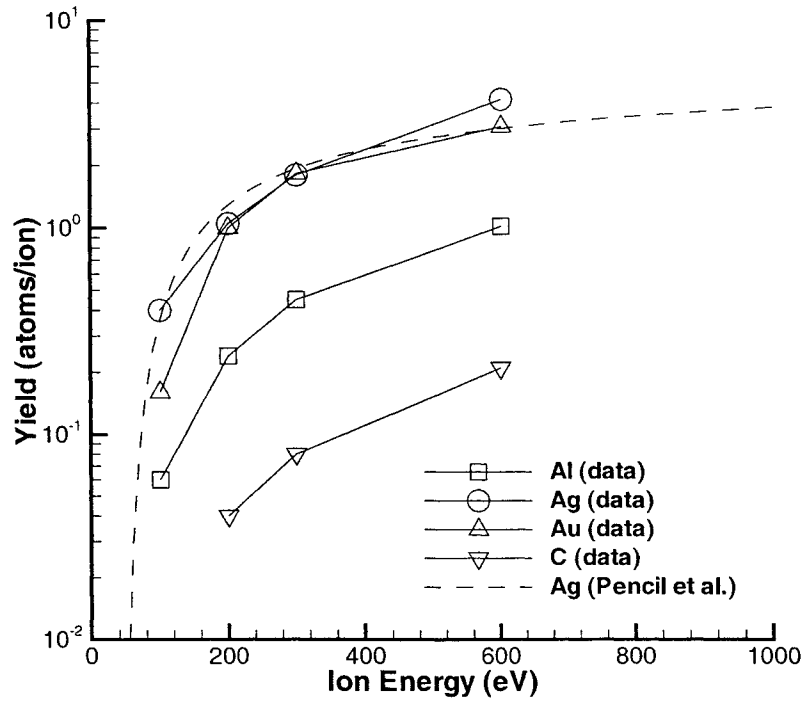


Fig. 1. Measured sputter yields for xenon ions at normal incidence.⁵

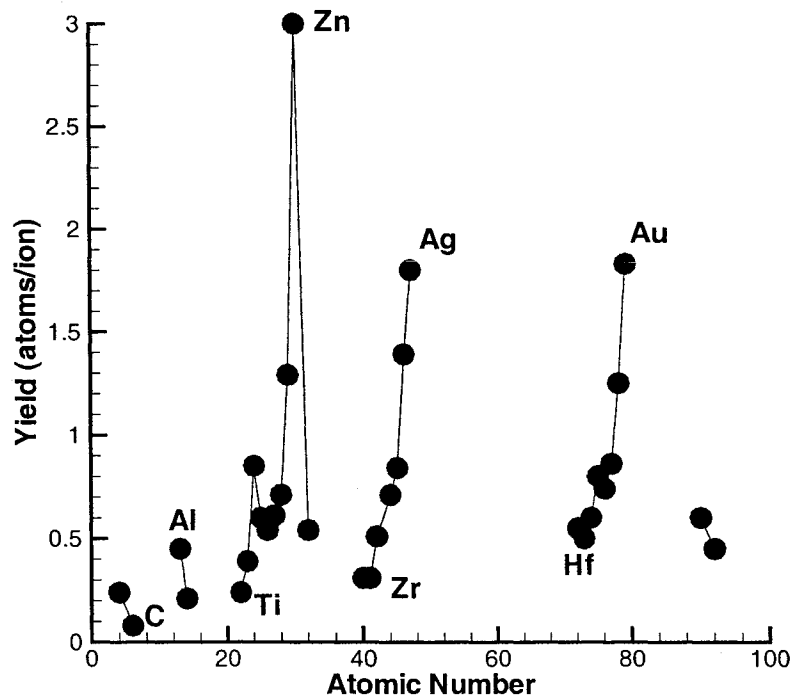


Fig. 2. Measured sputter yields for xenon ions at normal incidence at 300 eV.⁵

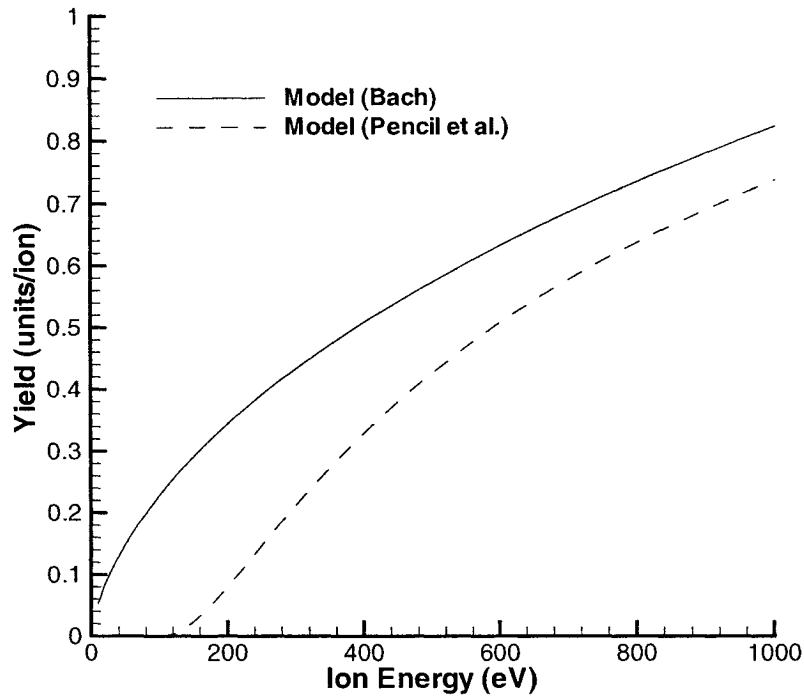


Fig. 3. Models^{6,8} of sputter yield for xenon ions at normal incidence on SiO₂.

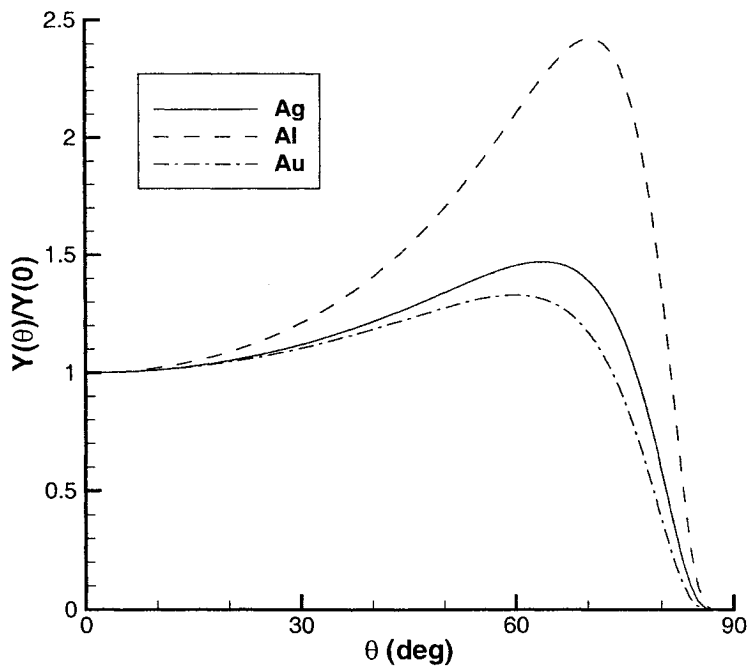


Fig. 4. Effect of incidence angle on sputter yield for argon ions at 1.05 keV on different metals using the model of Yamamura.¹³

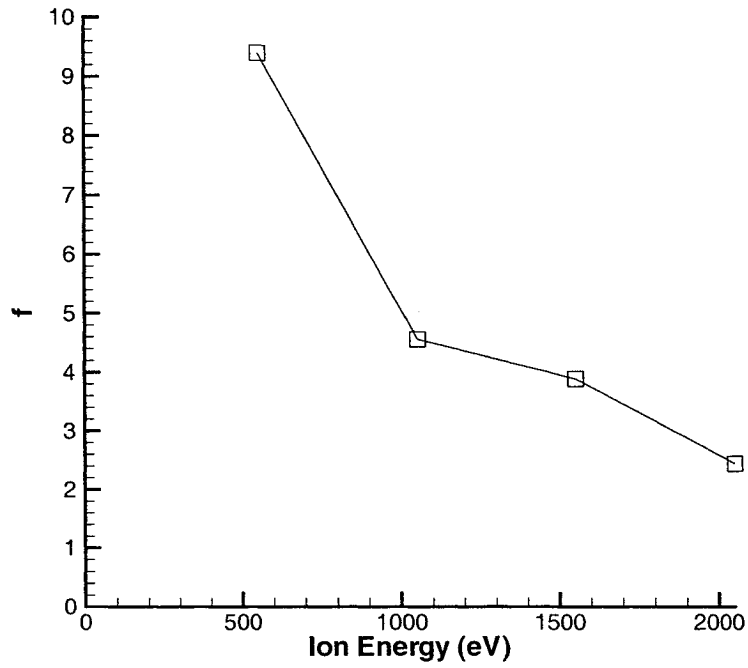


Fig. 5. Parameter f as a function of xenon ion energy impacting on copper.

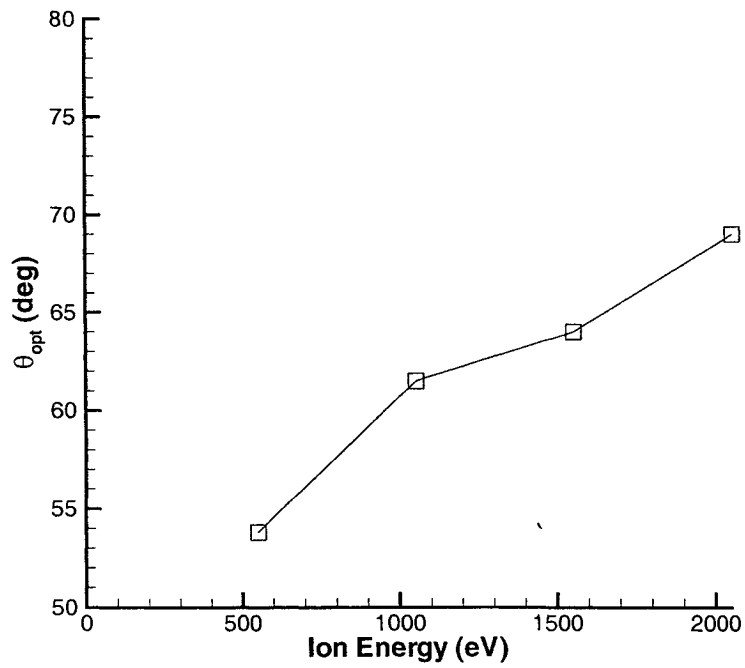


Fig. 6. Parameter θ_{opt} as a function of xenon ion energy impacting on copper.

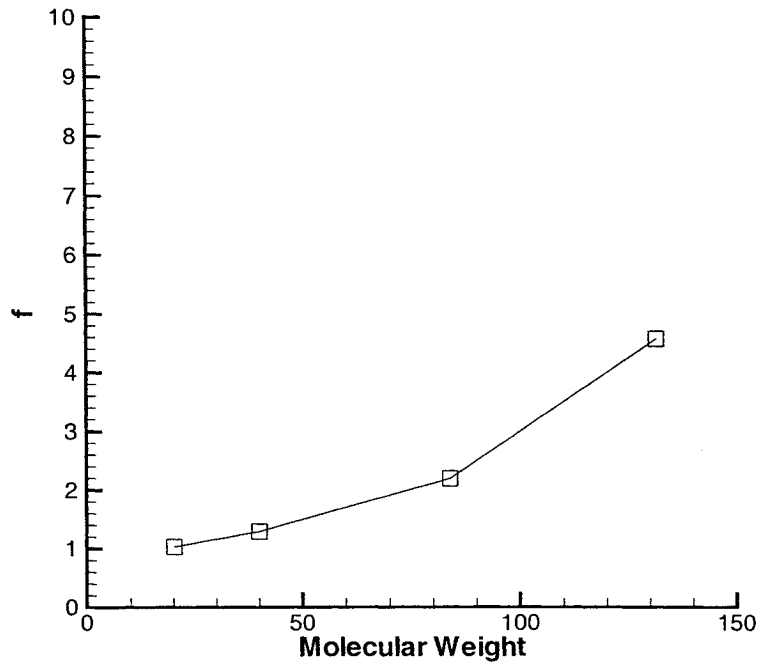


Fig. 7. Parameter f as a function of ion molecular mass for 1.05 keV impact on copper.

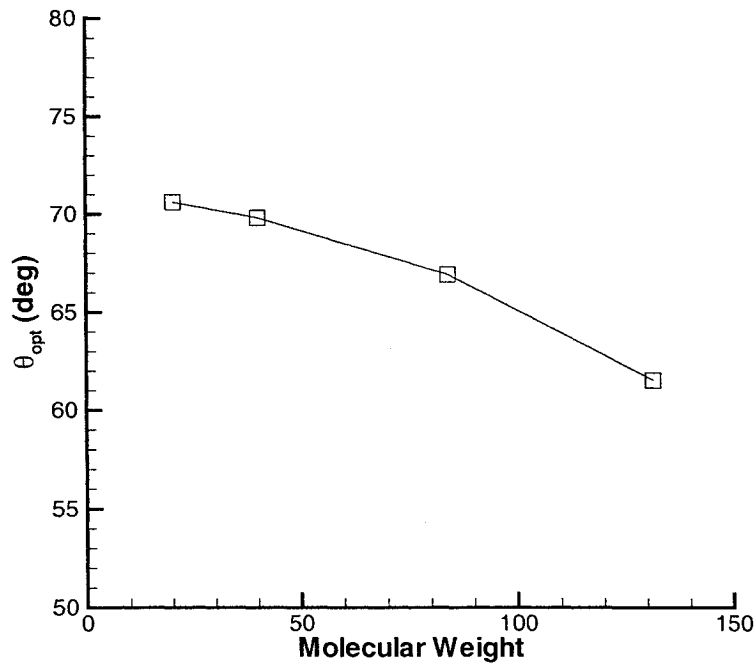


Fig. 8. Parameter θ_{opt} as a function of ion molecular mass for 1.05 keV impact on copper.

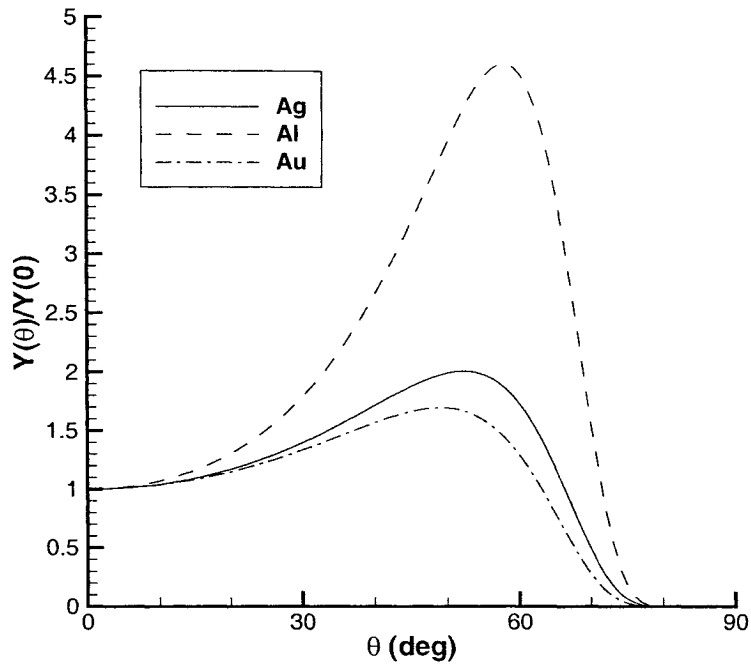


Fig. 9. Effect of incidence angle on sputter yield for xenon ions at 300 eV on different metals using the model of Yamamura¹³ (coefficients are listed in Table 2).

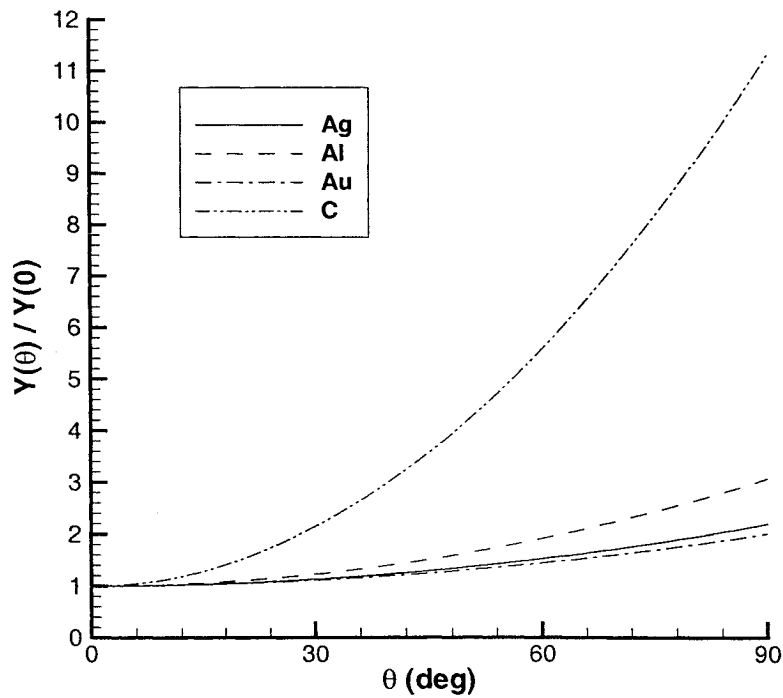


Fig. 10. Effect of angle of incidence on sputter yield for xenon ions at 300 eV using the model of Oechsner¹⁴.

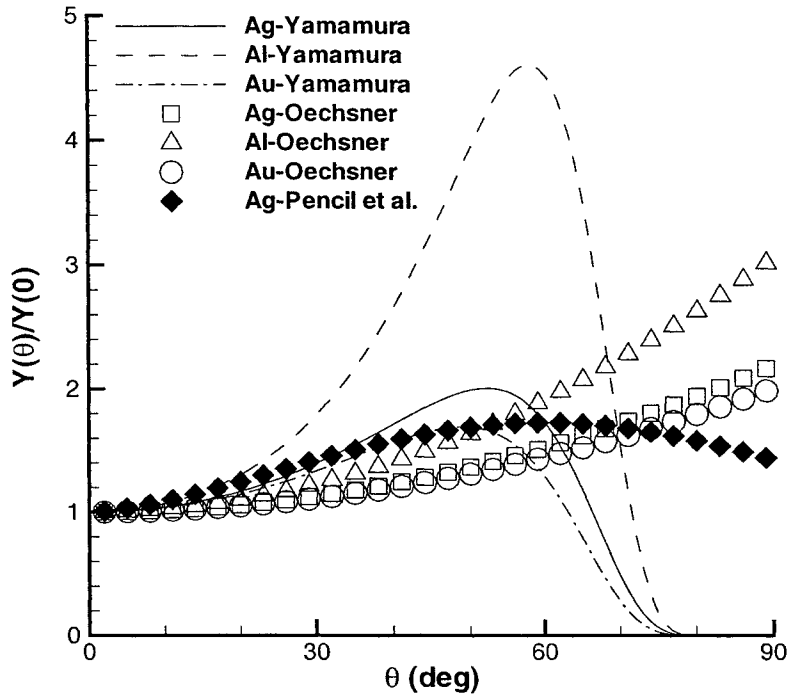


Fig. 11. Comparison of several models for xenon ions at 300 eV.

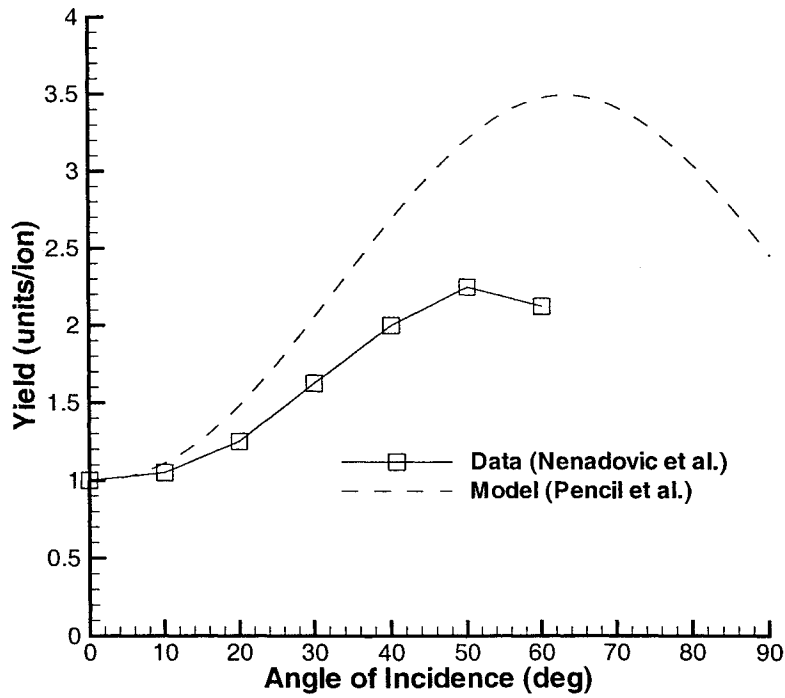


Fig. 12. Effect of angle of incidence on sputter yield of SiO₂.